



**HAL**  
open science

# Stochastic reduced-order model for an automotive vehicle in presence of numerous local elastic modes in the low-frequency range

A. Arnoux, Anas Batou, Christian Soize, L. Gagliardini

► **To cite this version:**

A. Arnoux, Anas Batou, Christian Soize, L. Gagliardini. Stochastic reduced-order model for an automotive vehicle in presence of numerous local elastic modes in the low-frequency range. International Conference on Uncertainty in Structural Dynamics (USD 2012), Katholieke Universiteit Leuven, Sep 2012, Leuven, Belgium. pp.4479-4488. hal-00734175

**HAL Id: hal-00734175**

**<https://hal.science/hal-00734175>**

Submitted on 20 Sep 2012

**HAL** is a multi-disciplinary open access archive for the deposit and dissemination of scientific research documents, whether they are published or not. The documents may come from teaching and research institutions in France or abroad, or from public or private research centers.

L'archive ouverte pluridisciplinaire **HAL**, est destinée au dépôt et à la diffusion de documents scientifiques de niveau recherche, publiés ou non, émanant des établissements d'enseignement et de recherche français ou étrangers, des laboratoires publics ou privés.

# Stochastic reduced-order model for an automotive vehicle in presence of numerous local elastic modes in the low-frequency range.

A. Arnoux<sup>1,2</sup>, A. Batou<sup>1</sup>, C. Soize<sup>1</sup>, L. Gagliardini<sup>2</sup>

<sup>1</sup> Université Paris-Est, Laboratoire Modélisation et Simulation Multi-Echelle,  
5 Boulevard Descartes, 77454 Marne-la Vallée, France  
e-mail: [adrien.arnoux@univ-mlv.fr](mailto:adrien.arnoux@univ-mlv.fr)

<sup>2</sup> PSA Peugeot Citroën, Direction Technique et Industrielle, Centre Technique de Vélizy A  
Route de Gisy, 78140 Vélizy Villacoublay, France

## Abstract

This paper is devoted to the construction of a stochastic reduced-order model for dynamical structures having a high modal density in the low-frequency range, such as an automotive vehicle. This type of structure is characterized by the fact that it exhibits, in the low-frequency range, not only the classical global elastic modes but also numerous local elastic modes which cannot easily be separated from the global elastic modes. To solve this difficult problem, an approach has recently been proposed for constructing a reduced-order computational dynamical model adapted to the low-frequency range. First, the domain of the structure is decomposed into subdomains. Then an adapted generalized eigenvalue problem is constructed using such a decomposition and allows an adapted vector basis of the global displacements space to be computed. This basis is then used to construct the reduced-order model. Model uncertainties induced by modeling errors in the computational model are taken into account using the nonparametric probabilistic approach. The methodology is applied on a complex computational model of an automotive vehicle.

## 1 INTRODUCTION

This work is performed in the context of the dynamic analysis of automotive vehicles. An automotive vehicle is made up of stiff parts and flexible components. In the low-frequency range, this type of structure is characterized by the fact that it exhibits, not only the classical global elastic modes, but also numerous local elastic modes in the same low-frequency band. With such a complex heterogeneous structure, the global elastic modes cannot clearly be separated from the local elastic modes because there are many small contributions of the local deformations in the deformations of the global elastic modes and conversely. Since there are local elastic modes in the low-frequency band, a part of the mechanical energy is transferred from the global elastic modes to the local elastic modes which store a part of mechanical energy and then this induces an apparent damping for the global coordinates. In order to construct a reduced-order model for the low-frequency band, which allows a good approximation of the global displacements to be predicted and then, if needed, to take into account the effects of the local displacements in the total response, a new approach [1] has recently been proposed. This method allows a basis of the global displacements space and a basis of the local displacements space to be calculated by solving two separated eigenvalue problems. This method that requires to decompose the computational model in subdomains for which the sizes are controlled. In this paper, we propose to use the Fast Marching Method for the construction of such subdomains. We construct a reduced-order model using only the basis of global displacements space. In addition, we introduce a stochastic reduced-order model in order to take into account the irreducible errors introduced by neglecting

the local displacements. In a first part, we present the construction of the stochastic reduced-order model. Then, we present the Fast Marching Method (see [2]). Finally, we apply the methodology for a complex Finite Element (FE) model of an automotive vehicle.

## 2 DESCRIPTION OF THE METHOD

In this section, we summarize the method introduced in [1]. This method allows a basis of the global displacements space and a basis of the local displacements space to be constructed by solving two separated eigenvalue problems. It should be noted that these two bases are not made up of the usual elastic modes. The method is based on the construction of a projection operator which reduces the kinetic energy while the elastic energy remains exact. This method is applied to the structural part of the vibroacoustic system we are interested in.

### 2.1 Reference computational model

We are interested in predicting the frequency response functions of a vibroacoustic damped structure occupying a domain  $\Omega$ , in the frequency band of analysis  $\mathcal{B} = [\omega_{\min}, \omega_{\max}]$  with  $0 < \omega_{\min}$ . Let  $\mathbb{U}(\omega)$  be the complex vector of the  $m$  DOF of the structural part of the vibroacoustic computational model constructed by the finite element method. Let  $[\mathbb{M}]$  and  $[\mathbb{K}]$  be the mass and stiffness matrices which are positive-definite symmetric ( $m \times m$ ) real matrices. The eigenfrequencies  $\lambda$  and the elastic modes  $\varphi$  in  $\mathbb{R}^n$  of the conservative part of the dynamical computational model of the structure are the solution of the following eigenvalue problem,

$$[\mathbb{K}] \varphi = \lambda [\mathbb{M}] \varphi . \quad (1)$$

Then an approximation  $\mathbb{U}_n(\omega)$  at order  $n$  of  $\mathbb{U}(\omega)$  can be written as

$$\mathbb{U}_n(\omega) = \sum_{\alpha=1}^n q_{\alpha}(\omega) \varphi_{\alpha} = [\Phi] \mathbf{q}(\omega) , \quad (2)$$

in which  $\mathbf{q}(\omega) = (q_1(\omega), \dots, q_n(\omega))$  is the complex vector of the  $n$  generalized coordinates and where  $[\Phi] = [\varphi_1 \dots \varphi_n]$  is the ( $m \times n$ ) real matrix of the elastic modes associated with the  $n$  first eigenvalues.

### 2.2 Decomposition of the domain for kinematic energy reduction.

In this section, we introduce a decomposition of the domain of the structure which allows a kinematic reduction of the kinetic energy to be performed. We then obtained an associated mass matrix which is adapted to the calculation of the global basis in the low-frequency band of analysis. The details of the methodology for the the continuous and the discrete cases are presented in [1].

#### 2.2.1 Decomposition of the domain $\Omega$

The domain  $\Omega$  is partitioned into  $n_J$  subdomains  $\Omega_j$  such that, for  $j$  and  $k$  in  $\{1, \dots, n_J\}$ ,

$$\Omega = \bigcup_{j=1}^{n_J} \Omega_j \quad , \quad \Omega_j \cap \Omega_k = \emptyset . \quad (3)$$

The choice of the length of subdomains is related to the smallest "wavelength" of the global vector basis that we want to extract in presence of numerous local modes. The construction of the subdomains are presented in Section 3.

## 2.2.2 Projection operator

Let  $\mathbf{u} \mapsto h^r(\mathbf{u})$  be the linear operator defined by

$$\{h^r(\mathbf{u})\}(\mathbf{x}) = \sum_{j=1}^{n_J} \mathbb{I}_{\Omega_j}(\mathbf{x}) \frac{1}{m_j} \int_{\Omega_j} \rho(\mathbf{x}') \mathbf{u}(\mathbf{x}') d\mathbf{x}', \quad (4)$$

in which  $\mathbf{x} \mapsto \mathbb{I}_{\Omega_j}(\mathbf{x}) = 1$  if  $\mathbf{x}$  is in  $\Omega_j$  and equal to 0 otherwise. The local mass  $m_j$  is defined, for all  $j$  in  $\{1, \dots, n_J\}$ , by  $m_j = \int_{\Omega_j} \rho(\mathbf{x}) d\mathbf{x}$ , where  $\mathbf{x} \mapsto \rho(\mathbf{x})$  is the mass density. Let  $\mathbf{u} \mapsto h^c(\mathbf{u})$  be the linear operator defined by

$$h^c(\mathbf{u}) = \mathbf{u} - h^r(\mathbf{u}). \quad (5)$$

Function  $h^r(\mathbf{u})$  will also be denoted by  $\mathbf{u}^r$  and function  $h^c(\mathbf{u})$  by  $\mathbf{u}^c$ . We then have  $\mathbf{u} = h^r(\mathbf{u}) + h^c(\mathbf{u})$  that is to say,  $\mathbf{u} = \mathbf{u}^r + \mathbf{u}^c$ . Let  $[H^r]$  be the  $(m \times m)$  matrix relative to the finite element discretization of the projection operator  $h^r$  defined by Eq. (4). Therefore, the finite element discretization  $\mathbb{U}$  of  $\mathbf{u}$  can be written as  $\mathbb{U} = \mathbb{U}^r + \mathbb{U}^c$ , in which

$$\mathbb{U}^r = [H^r] \mathbb{U}$$

and

$$\mathbb{U}^c = [H^c] \mathbb{U} = \mathbb{U} - \mathbb{U}^r, \quad ,$$

which shows that  $[H^c] = [I_m] - [H^r]$ . Then, the projected  $(m \times m)$  mass matrix  $[\mathbb{M}^r]$  is such that

$$[\mathbb{M}^r] = [H^r]^T [\mathbb{M}] [H^r], \quad ,$$

and the complementary  $(m \times m)$  mass matrix  $[\mathbb{M}^c]$  is such that

$$[\mathbb{M}^c] = [H^c]^T [\mathbb{M}] [H^c]. \quad .$$

Using the properties of the projection operator defined by Eq. (4), it can be shown [1] that

$$[\mathbb{M}^c] = [\mathbb{M}] - [\mathbb{M}^r]. \quad .$$

It should be noted that the rank of matrix  $[\mathbb{M}^r]$  is  $3n_J$ , and the rank of matrix  $[\mathbb{M}^c]$  is  $m - 3n_J$ .

## 2.3 Global and local displacements bases

There are two methods to calculate the global displacements basis and the local displacements basis. The first one is the direct method that will be used to reduce the matrix equation. In such a method, the basis of the global displacements space and the basis of the local displacements space are directly calculated using matrix  $[\mathbb{M}^r]$ . The second one, is the double projection. This method is less intrusive with respect to the commercial software and less time-consuming than the direct method. The global displacements eigenvectors  $\phi^g$  in  $\mathbb{R}^m$  are solution of the following generalized eigenvalue problem

$$[\mathbb{K}] \phi^g = \lambda^g [\mathbb{M}^r] \phi^g. \quad (6)$$

The local displacements eigenvectors  $\phi^\ell$  in  $\mathbb{R}^m$  are solution of the following generalized eigenvalue problem

$$[\mathbb{K}] \phi^\ell = \lambda^\ell [\mathbb{M}^c] \phi^\ell. \quad (7)$$

The solutions of the generalized eigenvalue problems defined by Eqs. (6) and (7) are then written, for  $n$  sufficiently large, as

$$\phi^g = [\Phi] \tilde{\phi}^g, \quad \phi^\ell = [\Phi] \tilde{\phi}^\ell, \quad (8)$$

in which  $[\Phi]$ , defined in Eq. (2), is the matrix of the elastic modes. The global displacements eigenvectors are the solutions of the generalized eigenvalue problem

$$[\tilde{K}] \tilde{\phi}^g = \lambda^g [\tilde{M}^r] \tilde{\phi}^g, \quad (9)$$

in which  $[\tilde{M}^r] = [\Phi^r]^T [\mathbb{M}] [\Phi^r]$  and  $[\tilde{K}] = [\Phi]^T [\mathbb{K}] [\Phi]$ , and where the  $(m \times n)$  real matrix  $[\Phi^r]$  is such that  $[\Phi^r] = [H^r] [\Phi]$ . The local displacements eigenvectors are the solutions of the generalized eigenvalue problem

$$[\tilde{K}] \tilde{\phi}^\ell = \lambda^\ell [\tilde{M}^c] \tilde{\phi}^\ell, \quad (10)$$

in which  $[\tilde{M}^c] = [\Phi^c]^T [\mathbb{M}] [\Phi^c]$  and where the  $(m \times n)$  real matrix  $[\Phi^c]$  is such that  $[\Phi^c] = [H^c] [\Phi] = [\Phi] - [\Phi^r]$ . It is proven in [1] that the family  $\{\phi_1^g, \dots, \phi_{3n_J}^g, \phi_1^\ell, \dots, \phi_{m-3n_J}^\ell\}$  is a basis of  $\mathbb{R}^m$ . The mean reduced matrix model is obtained by the projection of  $\mathbb{U}(\omega)$  on the family  $\{\phi_1^g, \dots, \phi_{n_g}^g, \phi_1^\ell, \dots, \phi_{n_\ell}^\ell\}$  of real vectors associated with the  $n_g$  first global displacements eigenvectors such that  $n_g \leq 3n_J < m$  and with the  $n_\ell$  first local displacements eigenvectors such that  $n_\ell < m - 3n_J$ . It should be noted that, if the double projection method is used, then we must have  $n_g + n_\ell \leq n$ . Then, the approximation  $\mathbb{U}_{n_g, n_\ell}(\omega)$  of  $\mathbb{U}(\omega)$  at order  $(n_g, n_\ell)$  is written as

$$\mathbb{U}_{n_g, n_\ell}(\omega) = \sum_{\alpha=1}^{n_g} q_\alpha^g(\omega) \phi_\alpha^g + \sum_{\beta=1}^{n_\ell} q_\beta^\ell(\omega) \phi_\beta^\ell. \quad (11)$$

This decomposition is then used to construct the generalized mass, stiffness and damping matrices which can be written in a block representation as

$$[\mathbb{M}] = \begin{pmatrix} M^{gg} & M^{gl} \\ M^{lg} & M^{ll} \end{pmatrix}, \quad [\mathbb{D}] = \begin{pmatrix} D^{gg} & D^{gl} \\ D^{lg} & D^{ll} \end{pmatrix}, \quad [\mathbb{K}] = \begin{pmatrix} K^{gg} & K^{gl} \\ K^{lg} & K^{ll} \end{pmatrix}. \quad (12)$$

## 2.4 Mean reduced model adapted to the low-frequency range

The objective of this work is to construct a reduced-order model adapted to the low-frequency range in which the synthesis of the frequency responses is obtained using only the global displacements eigenvectors. So the new approximation  $\mathbb{U}_{n_g}(\omega)$  of  $\mathbb{U}(\omega)$  at order  $n_g$  is written as

$$\mathbb{U}_{n_g}(\omega) = \sum_{\alpha=1}^{n_g} q_\alpha^g(\omega) \phi_\alpha^g. \quad (13)$$

The corresponding reduced-order matrix equation is then written as

$$(-\omega^2 [M^{gg}] + i\omega [D^{gg}] + [K^{gg}]) \mathbf{q}^g = \mathbf{f}^g. \quad (14)$$

Since a part of the mechanical energy is transferred from the global coordinates to the local coordinates and which induces an apparent damping, we propose to replace the generalized damping matrix  $[D^{gg}]$  by a modified damping matrix  $[D_{mod}^{gg}]$  which is calculated by minimizing the distance between the frequency responses computed with the proposed reduced-order model and the frequency responses given by the reference model.

## 2.5 Probabilistic model of uncertainties

A probabilistic model of uncertainties is introduced in the reduced-order computational model in order to take into account the system-parameter uncertainties and the model uncertainties induced by modeling errors in the reference model from which the reduced-order model has been deduced. We also have to take into

account uncertainties induced by the irreducible errors introduced by neglecting the contribution of the local displacements in the constructed reduced-order model. To take into account all these sources of uncertainties, we use the nonparametric probabilistic approach (see [4]) which consists in replacing, in the reduced-order computational model, the deterministic generalized mass, damping and stiffness matrices by random matrices. In this work, the uncertainties are not taken into account on the modified generalized damping matrix (it has previously been proven that the random frequency responses are not sensitive to the statistical fluctuations of the damping matrix in the framework of the nonparametric probabilistic approach). Therefore the matrices  $[M^{gg}]$  and  $[K^{gg}]$  are replaced by the random matrices  $[\mathbf{M}^{gg}]$  and  $[\mathbf{K}^{gg}]$  for which the probability density functions (PDF) and the generator of independent realizations are given in [4]. The PDF of these two random matrices depend on two dispersion parameters ( $\delta_{M^{gg}}$  and  $\delta_{K^{gg}}$ ) which have to be identified using the random frequency response of the stochastic reference model and the maximum likelihood method. Therefore, the random frequency response of the stochastic reduced-order model,  $\mathbf{U}^g(\omega; \delta_{M^{gg}}; \delta_{K^{gg}})$ , is solution of the equation

$$\mathbf{U}^g(\omega; \delta_{M^{gg}}; \delta_{K^{gg}}) = \sum_{\alpha=1}^{n_g} \mathbf{Q}^\alpha(\omega; \delta_{M^{gg}}; \delta_{K^{gg}}) \phi^\alpha, \quad (15)$$

$$(-\omega^2[\mathbf{M}^{gg}(\delta_{M^{gg}})] + i\omega[D_{mod}^{gg}] + [\mathbf{K}^{gg}(\delta_{K^{gg}})])\mathbf{Q}^g(\omega; \delta_{M^{gg}}; \delta_{K^{gg}}) = \mathbf{f}^g. \quad (16)$$

### 3 CONSTRUCTION OF THE SUBDOMAINS

For the computational model of a complex structure such as an automotive vehicle, the decomposition of the domain is not easy to be carried out because the geometry is very complex and curved. The method we propose for this decomposition is based on the Fast Marching Methods (FMM) introduced in [2] which gives a way to propagate a front (the notion of front will be defined below) on connected parts from a starting point. In this section, the FMM is summarized and then we explain how to construct the subdomains using the FMM.

#### 3.1 Presentation of the Fast Marching Method (FMM)

Let  $\mathbf{x}$  be the generic point in  $\mathbb{R}^3$  belonging to the complex geometry  $\Omega$ . Let  $\mathbf{x}_0$  be a fixed point belonging to  $\Omega$ . Let  $U(\mathbf{x})$  be a geodesic distance adapted to the geometry, between  $\mathbf{x}$  and  $\mathbf{x}_0$ . It should be noted that for a simple 3D volume domain, such a geodesic distance would be the Euclidean distance  $\|\mathbf{x} - \mathbf{x}_0\|$  in which  $\|\cdot\|$  is the Euclidean norm. The front related to  $\mathbf{x}_0$  is defined as the subset of all the  $\mathbf{x}$  such that  $U(\mathbf{x})$  has a fixed value. The FMM [2] allows the front to be propagated from starting point  $\mathbf{x}_0$ . We then have to calculate  $U(\mathbf{x})$  verifying the following nonlinear Eikonal equation

$$\|\nabla U(\mathbf{x})\| = F(\mathbf{x}) \quad , \quad \mathbf{x} \in \Omega \quad , \quad (17)$$

with  $\nabla$  the gradient with respect to  $\mathbf{x}$ , in which  $F(\mathbf{x})$  is a given arbitrary positive-valued function and for which the boundary condition is written as  $U(\mathbf{x}) = 0$  on  $\Gamma_0$  which is a curved line or a surface containing  $\mathbf{x}_0$ . Introducing the finite element mesh of  $\Omega$ , Eq. (17) is discretized using an *upwind* approximation (forward finite difference) for the gradient (see [2]). For the particular case of a rectangular regular finite element mesh for which the mesh size is  $h$  and for which the nodes are  $\mathbf{x}_{ij}$ , we have to find  $U_{ij} = U(\mathbf{x}_{ij})$  as the solution of the following equation

$$\begin{aligned} & \{\max(U_{ij} - U_{i-1,j}, U_{ij} - U_{i+1,j}, 0)\}^2 \\ & + \{\max(U_{ij} - U_{i,j-1}, U_{ij} - U_{i,j+1}, 0)\}^2 = h^2 F_{ij}^2. \end{aligned} \quad (18)$$

Since the information in Eq. (18) propagates in a unique way, this equation allows the front to be propagated from the starting point. The use of the word *Fast* in FMM is due to the fact that the nodes associated with  $U_{ij}$  and identified by Eq. (18) belong to a small domain which is called the Narrow Band (NB).

In the FMM, the algorithm introduces three groups of nodes:

- (1) *alive* nodes for which the value of  $U_{ij}$  is fixed and does not change,
- (2) *trial* nodes for which the value of  $U_{ij}$  is given but has to be updated until they become *alive* and these nodes constitute the Narrow Band,
- (3) *far* nodes which have not been reached by the front and therefore are such that  $U_{ij} = +\infty$ .

The front is propagated using the following algorithm:

#### *Initialization*

- Choose a starting node  $\mathbf{x}_0$  rewritten as  $\mathbf{x}_{0,0}$ , which is *alive* and set  $U_{0,0} = U(\mathbf{x}_{0,0}) = 0$ .
- The 4 neighboring nodes of  $\mathbf{x}_{0,0}$  become *trial* nodes and the associated value of  $U$  is set to  $hF_{ij}$ .
- All the other nodes are *far* nodes with associated value of  $U$  equal to infinity.

#### *Loop*

- Search among *trial* nodes, the node  $\mathbf{x}_{ij}$  with the smallest value of  $U$ .
- Remove  $\mathbf{x}_{ij}$  from *trial* nodes and add  $\mathbf{x}_{ij}$  to *alive* nodes.
- For each neighboring node of  $\mathbf{x}_{ij}$ , there are two possible cases:
  - if the neighboring node is a *far* node, add it to the *trial* nodes and its value of  $U$  is set to  $U_{ij} + hF_{ij}$ .
  - if the neighboring node is a *trial* node, its value of  $U$  is updated solving Eq. (18).

The loop is repeated until all the node are *alive*. For triangular meshes, the algorithm described above is unchanged but Eq. (18) must be adapted (see [3]).

### **3.2 Construction of the subdomains**

The subdomains  $\{\Omega_j, j = 1, \dots, n_J\}$  of  $\Omega$  are constructed using the FMM. This construction has two steps. The first one consists in choosing the centers of the subdomains. The second one consists in generating the subdomains using these centers as starting points.

#### *(i) Selection of the subdomains centers*

The subdomains centers are chosen on the stiff parts of the computational model and are uniformly distributed on the stiff parts.

#### *(ii) Computation of the subdomains*

To construct the subdomains  $\{\Omega_j, j = 1, \dots, n_J\}$  for which the subdomains centers have previously been chosen, we simultaneously propagate a front starting from each center until all the nodes become *alive* nodes with respect to one of the front. Then, the boundaries of the subdomains correspond to the meeting lines of the fronts.

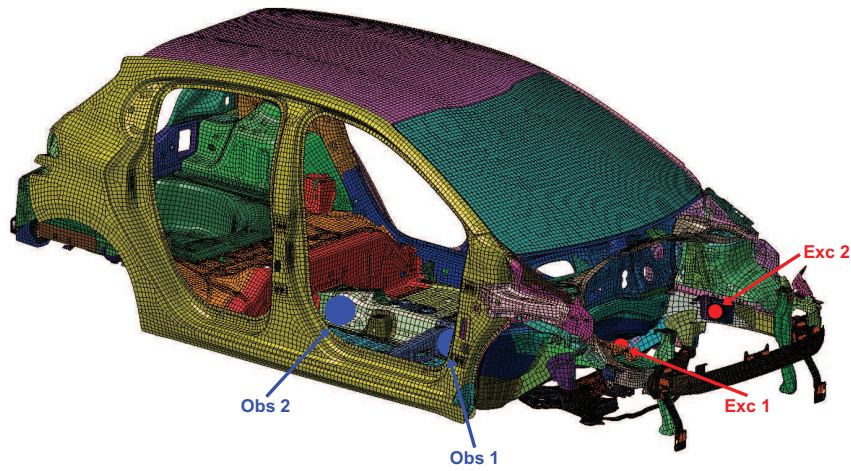


Figure 1: The Finite Element model of an automotive vehicle

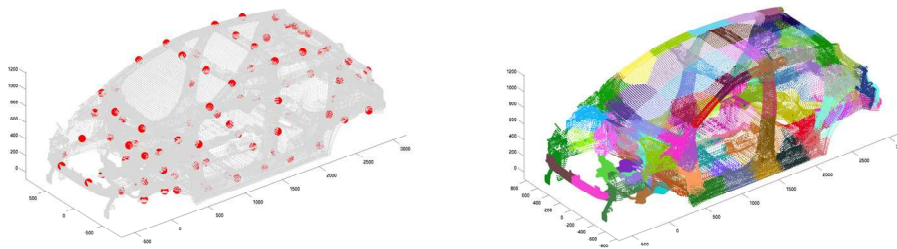


Figure 2: Centers of the subdomains (left) and subdomains (right)

## 4 APPLICATION

In this section, we present an application of the methodology presented in the previous sections for a complex real automotive model.

### 4.1 Presentation

The application is done for a computational model (FE Model) of an automotive vehicle. Such a FE model has 250 000 nodes and contains various types of finite elements such as volume finite elements, surface finite elements and beam elements. The frequency band of analysis is  $\mathcal{B} = ]0, 120] Hz$ . The structure has 1, 462, 698 DOF.

#### 4.1.1 Decomposition of the domain

The FMM method presented in Section 3 is applied to the mesh of the structure of the automotive model. The centers of the subdomains and the subdomains obtained from these centers are represented in Fig. 2.

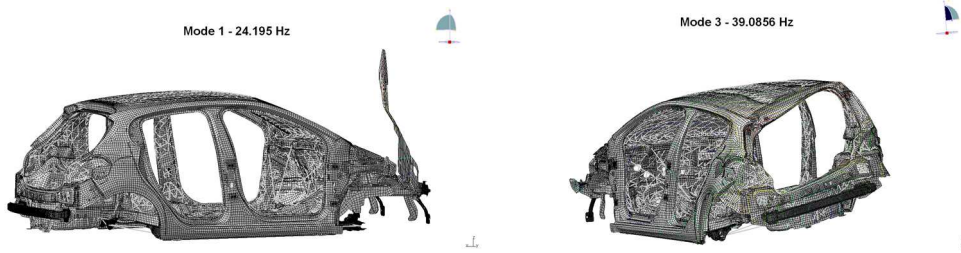


Figure 3: First elastic mode (left) and third elastic mode (right).

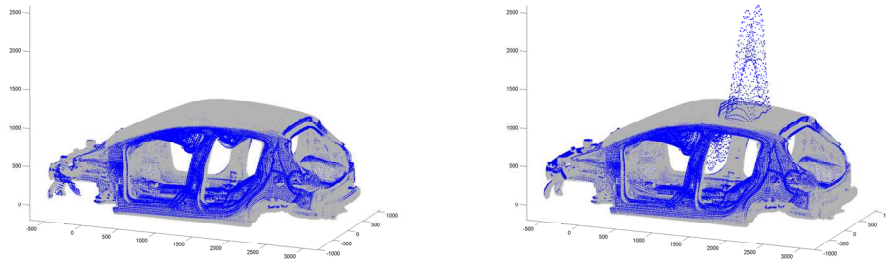


Figure 4: Fourth global displacements eigenvector (left) and corresponding eleventh elastic mode (right).

#### 4.1.2 Elastic modes, global and local displacements eigenvectors

In a first step, the elastic modes are calculated with the finite element model. There are 160 eigenfrequencies in the frequency band of analysis  $\mathcal{B}$ . The first elastic mode  $\phi_1$  and the third elastic mode  $\phi_3$  are displayed in Fig. 3 which shows that  $\phi_1$  is a local elastic mode while  $\phi_{11}$  is a global elastic mode with an important local displacement (see Fig. 4). In a second step, the global and local displacements eigenvectors are constructed using the double projection method. In frequency band  $]0, 120[ Hz$ , there are  $n_g = 36$  global displacements eigenvectors and  $n_\ell = 124$  local displacements eigenvectors. To see the good separation obtained between the global displacements eigenvectors and the local displacements eigenvectors, Fig. 4 displays the eleventh elastic mode (right figure) for which there are local displacements and the corresponding fourth global displacements eigenvector (left figure) for which the local displacements have been filtered.

### 4.2 Frequency response functions

For all  $\omega \in \mathcal{B}$ , the structure is subjected to an external point load equal to 1 N applied to two nodes, Exc1 and Exc2, located in the stiff part of the structure. The frequency response is calculated at two observation points, Obs<sub>1</sub> and Obs<sub>2</sub>, which are located in the stiff part (see Fig. 1). The frequency responses are calculated for different projections associated with the different bases: for the elastic modes ( $n = 160$ ), for global displacements eigenvectors ( $n_g = 36$  and  $n_\ell = 0$ ) and finally, for global displacements eigenvectors with the modification of the damping matrix ( $n_g = 36$  and  $n_\ell = 0$ ) and for global and local displacements eigenvectors ( $n_g = 36$  and  $n_\ell = 124$ ). The modulus, in log scale, of the frequency response function is displayed in Fig. 5. It can be seen that the responses calculated using global and local displacements eigenvectors are exactly the same that the response calculated using the elastic modes. In the Fig. 5, we can see that for each observation node, the response calculate with the global displacement eigenvector gives a good approximation of the response calculate with the elastic modes. Moreover, the response calculated with the modified damping matrix gives a better result.

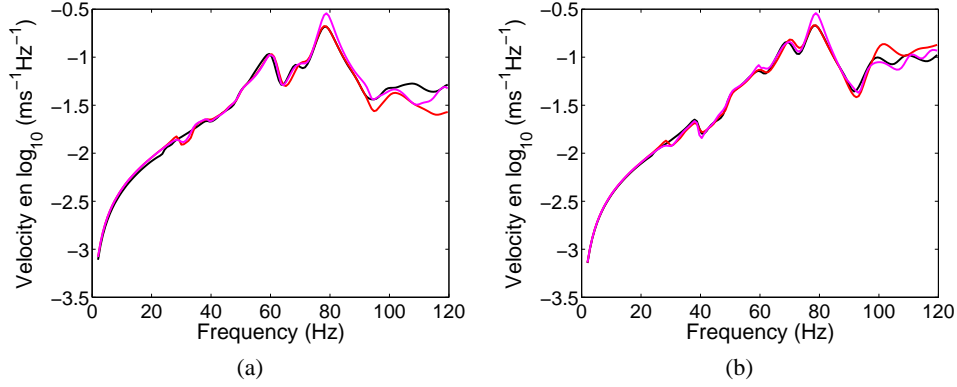


Figure 5: Modulus, in log scale, of the frequency response function for  $\text{Obs}_1$  (a) and  $\text{Obs}_2$  (b). Comparisons between different projection bases: elastic modes (black solid thick line), global displacements eigenvectors only (red solid thick line), global displacements eigenvectors with modification of the damping matrix (magenta solid thick line), global and local displacements eigenvectors (solid thin line superimposed to the solid thick line).

### 4.3 Random frequency response

The stochastic reference computational model is thus constructed with the reference computational model presented in Section 2.1, using the nonparametric probabilistic approach of uncertainties as explained in [5]. The values of the dispersion parameters  $\delta_{\mathbb{M}}^{ref}$  (for the random matrix  $\mathbb{M}$ ) and  $\delta_{\mathbb{K}}^{ref}$  (for the random matrix  $\mathbb{K}$ ) are those identified in [5]. All the calculations are carried out with the Monte Carlo simulation method for which 1,000 independent realizations are used. The confidence regions corresponding to a probability level  $P_c = 0.95$  is plotted in Fig. 6(a) and Fig. 6(b) (dark grey regions).

We then have calculated the random frequency responses using the stochastic reduced-order model. All the calculations are carried out with the Monte Carlo simulation method for which 1,000 independent realizations are used. The first step consists in calculating the optimal values of the dispersion parameters  $\delta_{M^{gg}}^{opt}$  (for the random matrix  $M^{gg}$ ) and  $\delta_{K^{gg}}^{opt}$  (for the random matrix  $K^{gg}$ ) using the maximum likelihood method. For these optimal values of the dispersions parameters, the confidence regions corresponding to a probability level  $P_c = 0.95$  are plotted in Fig. 6(a) and Fig. 6(b) (magenta regions) for  $\text{Obs}_1$  and  $\text{Obs}_2$ . For each observation points, the confidence region calculated with the reference computational model is included in the confidence region calculated with the stochastic reduced-order model. The amplitude of the confidence region calculated with the stochastic reduced-order model is larger than the one calculated with the stochastic reference computational model. This is due to the fact that the first one takes into account both the model uncertainties and the uncertainties induced by the construction of the reduced-order model adapted to the low-frequency range for which the local contributions have been removed, while the second one only takes into account the model uncertainties and for which the local contributions have not been removed.

## 5 CONCLUSION

In this work, we have applied a new methodology allowing a reduced-order computational dynamical model to be constructed for the low-frequency domain in which there are simultaneously global and local elastic modes which cannot easily be separated with usual methods. Moreover, we have used the Fast Marching Method which is adapted to complex geometry for constructing the subdomains and the adapted reduced-order computational model. An associated stochastic reduced-order model has then been introduced to take

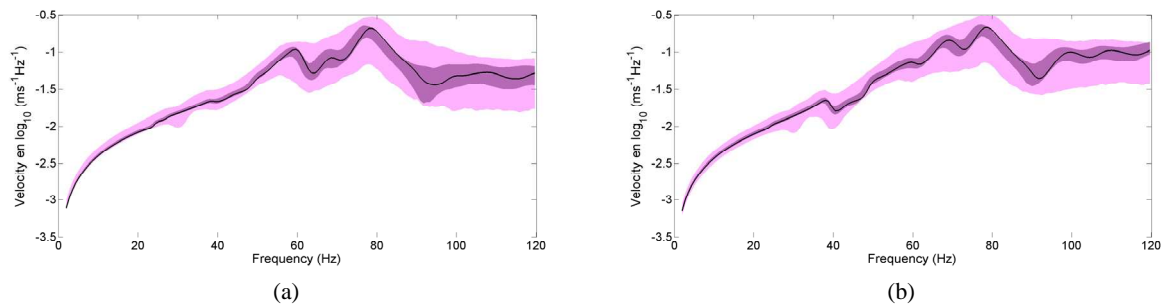


Figure 6: Modulus, in log scale, of the random frequency response function for Obs<sub>1</sub> (a) et Obs<sub>2</sub> (b). Confidence region (dark gray region) computed with the reference computational model. Confidence region (magenta region) computed with the stochastic reduced-order model. Deterministic response calculate the elastic modes (black solid thick line)

into account uncertainties in the adapted reduced-order model. The results obtained are good with respect to the objectives fixed in this work consisting in constructing a reduced-order model with a very low dimension, which has the capability to predict the frequency responses of the stiff part, in the low-frequency range.

## References

- [1] C. Soize and A. Batou, Stochastic reduced-order model in low frequency dynamics in presence of numerous local elastic modes, *Journal of Applied Mechanics - Transaction of the ASME*, 78(6): 061003, 2011.
- [2] J.A. Sethian, A Fast Marching Level Set Method for Monotonically Advancing Fronts, *Proc. Nat .Acad. Sci.*, 93, 4, 1996.
- [3] J.A. Sethian and R. Kimmel, Computing Geodesic Paths on Manifolds, *Proc. Nat .Acad. Sci.*, 95, 8431-8435, 1998.
- [4] C. Soize, A nonparametric model of random uncertainties for reduced matrix models in structural dynamics, *Probabilistic Engineering Mechanics*, 15(3) :277-294, 2000.
- [5] J.F Durand, C. Soize, L. Galiardini, Structural-acoustic modeling of automotive vehicles in presence of uncertainties and experimental identification and validation, *Journal of the Acoustical Society of America*, 124(3) (2008) 1513-1525.